First publ. in: Advanced Functional Materials ; 22 (2012), 10. - S. 2202-2208

http:/dx.doi.org/10.1002/adfm.201102263

Incompatible Length Scales in Nanostructured Cu_2O Solar Cells

Kevin P. Musselman, Andrew Marin, Lukas Schmidt-Mende, and Judith L. MacManus-Driscoll**

Electrodeposited Cu_2O-ZnO heterojunctions are promising low-cost solar cells. While nanostructured architectures improve charge collection in these devices, low open-circuit voltages result. Bilayer and nanowire Cu_2O-ZnO heterojunction architectures are systematically studied as a function of the Cu_2O layer thickness, ZnO nanowire length, and nanowire seed layer. It is shown that a thick depletion layer exists in the Cu_2O layer of bilayer devices, owing to the low carrier density of electrodeposited Cu_2O, such that the predominant charge transport mechanisms in the Cu_2O and ZnO are drift and diffusion, respectively. This suggests that the low open-circuit voltage of the nanowire cells is due to an incompatibility between the nanostructure spacing required for good charge collection (<1 μm) and the heterojunction thickness necessary to form the full built-in potential that inhibits recombination (>2 μm). The work shows the way to improve low-cost Cu_2O cells: increasing the carrier concentration or mobility in Cu_2O synthesized at low temperatures.

1. Introduction

Inexpensive solar cells that can be synthesized from solutions near room temperature on a variety of low-cost substrates are highly desired for distributed electricity generation. Several favorable characteristics such as material abundance, low-toxicity, and stability have been identified for these "ultra-low-cost" cells and all-oxide photovoltaics have the potential to meet these requirements.[1,2] However, due to the smaller grain sizes and inferior crystalline perfection of semiconductors synthesized from solutions, lower mobilities and shorter collection lengths are expected for photogenerated charges in such devices. Nanostructured architectures have been employed to address the short collection lengths,[1,3–7] but inadequate consideration has often been given to the influence of such structures on the underlying device physics. In this work, the manner in which nanostructured heterojunctions influence the performance of all-oxide Cu_2O-ZnO photovoltaics is reported and, for the first time, fundamental limitations of such devices are identified.

Cuprous oxide has been recognized as a promising photovoltaic (PV) material due to its abundance, high theoretical power conversion efficiency (η) of around 20%, and ability to be electrochemically synthesized from solution.[2,8,9] The intrinsically p-type nature, self-compensation problems, and low dopant solubility have inhibited the synthesis of n-type Cu_2O to give efficient homojunctions.[10,11] Heterojunction architectures have therefore been employed with various n-type window layers, of which ZnO has been found to be most stable and efficient.[12–15] Despite the high theoretical η values of Cu_2O, experimental efficiencies have yet to reach 2% for electrochemically synthesized Cu_2O-ZnO devices. Open-circuit voltages (V_{OC}) of the best solution-synthesized bilayer devices have approached 0.6 V, close to the expected Fermi level offset in the two materials.[14] However, the short-circuit current densities (J_{SC}) reported for these cells (less than 4 mA cm^{-2} under standard illumination)[14,16] are well below the value of approximately 15 mA cm^{-2} expected from the bandgap of Cu_2O,[3] indicating that charge collection currently limits the performance of electrodeposited bilayer devices. Nanostructured heterojunctions utilizing ZnO nanowires and nanotubes have been used to improve charge collection and increase the J_{SC} of electrodeposited Cu_2O-ZnO cells,[3–7] however, the V_{OC} and η of these nanostructured cells were less than those of the best bilayer devices.

In this work, the performance of bilayer and nanowire (NW) Cu_2O-ZnO solar cells is systematically studied as a function of the thickness of the Cu_2O absorbing layer, ZnO NW length, and NW seed layer. A greater understanding of the underlying device physics is obtained. It is suggested that the inferior performance of the nanostructured heterojunctions is due to an incompatibility between the large length scale required for formation of the built-in bias and the short length scale required for efficient charge collection. It is explained that this incompatibility arises from the low carrier concentration and low mobility of electrodeposited Cu_2O, and materials improvements required to simultaneously achieve high J_{SC}'s and V_{OC}'s in solution-processed Cu_2O photovoltaics are outlined.

Dr. K. P. Musselman, A. Marin,
Prof. J. L. MacManus-Driscoll
Department of Materials Science
University of Cambridge
Pembroke St., Cambridge, CB2 3QZ, UK
E-mail: kpdm2@cam.ac.uk; jld35@cam.ac.uk
Prof. L. Schmidt-Mende
Department of Physics and Center for Nanoscience (CeNS)
Ludwig-Maximilians University
Amalienstr. 54, 80799 Munich, Germany

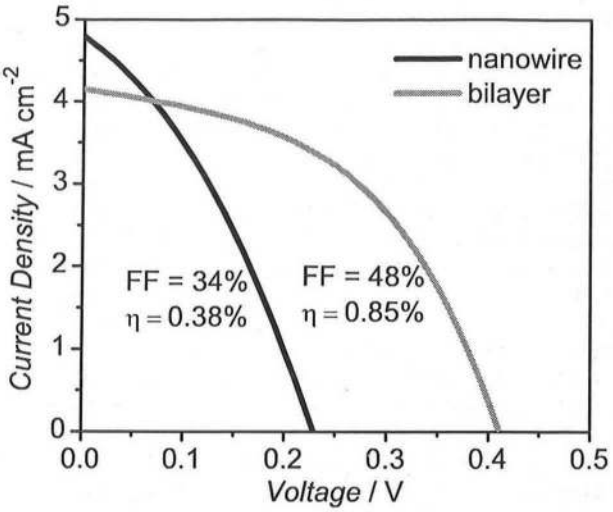

Figure 1. Solar simulator measurements for bilayer and NW electrodeposited Cu_2O-ZnO solar cells (AM1.5, 100 mW cm^{-2} illumination).

2. Results and Discussion

Figure 1 displays solar simulator measurements of a bilayer and nanowire Cu_2O-ZnO cell. Schematics of the cell architectures are shown in **Figure 2**a,b. Both devices in Figure 1 have an approximately 3 μm thick Cu_2O absorbing layer and the ZnO NWs have a nominal length of 1.25 μm. While the nanostructured architecture improves the J_{SC} of the NW cell, a dramatically lower V_{OC} is obtained. To our knowledge, the greatest η values measured for nanostructured Cu_2O-ZnO cells under standard illumination are approximately 0.5 to 0.6%,[16,17] significantly lower than that observed in equivalent bilayer cells.[14,16]

2.1. Interface Effects and Leakage Paths

A reduction in V_{OC} from the theoretical value is a common feature of nanostructured photovoltaics, and has often been attributed to leakage paths and/or to an increase in recombination at the larger interfacial area.[1,5,18] To examine the possibility of leakage paths through the approximately 50 nm ZnO NW seed layer, a third device architecture was also examined, as illustrated in **Figure 3**a. A ZnO thin film, like that used in the bilayer device of Figure 2a, was first synthesized. A sputter-coated ZnO seed layer and ZnO NWs (nominal length 500 nm) were then deposited on top of the ZnO film, in an identical manner as for the NW cells. Finally, a similar 3 μm Cu_2O layer and top contacts were deposited. This results in a nanostructured ZnO-Cu_2O interface similar to that of the NW cells, on top of a continuous 550 nm ZnO film like that employed in the bilayer devices. Figure 3b shows a scanning electron microscopy (SEM) image of the ZnO NWs grown on top of the grains of the ZnO film.

In Figure 3c, the dark current density of this device architecture is shown, along with that of the bilayer and NW cells of Figure 1. The composite architecture of Figure 3a does exhibit a slightly smaller dark current density than the NW cell at small reverse biases, which suggests that the presence of the underlying ZnO film may prevent a small amount of leakage current which would otherwise pass through the thin ZnO seed layer. However, the performance of the composite architecture is much more similar to the NW cell than the bilayer device, especially at small positive biases. This strongly suggests that the increased recombination and lower V_{OC} observed in the NW cells is not due to shunting through the approximately 50 nm thick ZnO seed layer, but is instead intrinsic to the nanostructured heterojunction. NW cells were also synthesized with thicker ZnO seed layers and no improvement in performance was observed.

Modeling of radial p-n junction nanorod solar cells has indicated that the V_{OC} could decrease with increasing NW length, as the junction area and recombination current are increased.[19] To examine the influence of the heterojunction area on the performance of Cu_2O-ZnO NW cells, devices were fabricated with approximately 3 μm of Cu_2O and different nominal NW lengths. Three devices were measured for each NW length and their V_{OC}'s are summarized in **Table 1** (standard deviation given by the error bounds). No decrease in V_{OC} is observed with increasing NW length. **Figure 4** displays dark current measurements for typical devices with these NW lengths. No clear increase in dark current density is observed with increasing interfacial area. At reverse bias, the device with a nominal NW length of 575 nm, which is expected to have the smallest interfacial area, shows the largest dark current. This might be

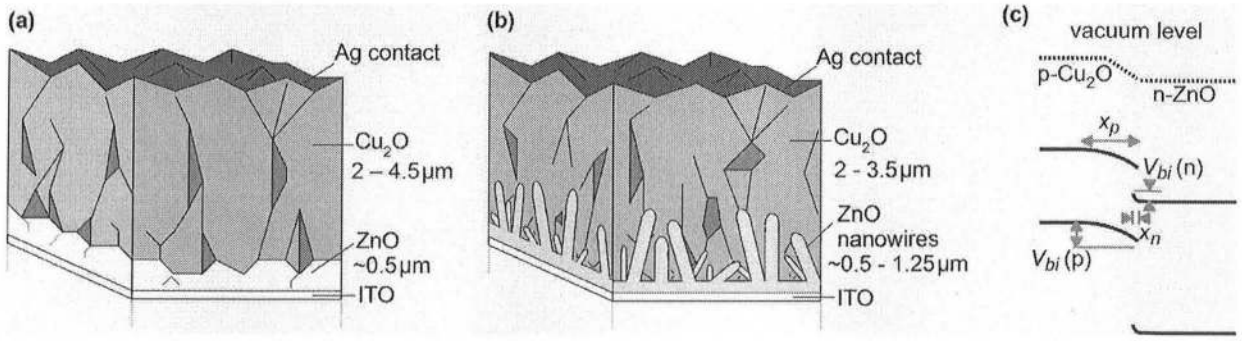

Figure 2. Schematic diagrams of bilayer (a) and NW (b) Cu_2O-ZnO solar cell architectures studied in this work. c) Energy level diagram of Cu_2O-ZnO heterojunction with components of the built-in bias ($V_{bi}(p)$, $V_{bi}(n)$) and depletion layer thicknesses (x_p,x_n).

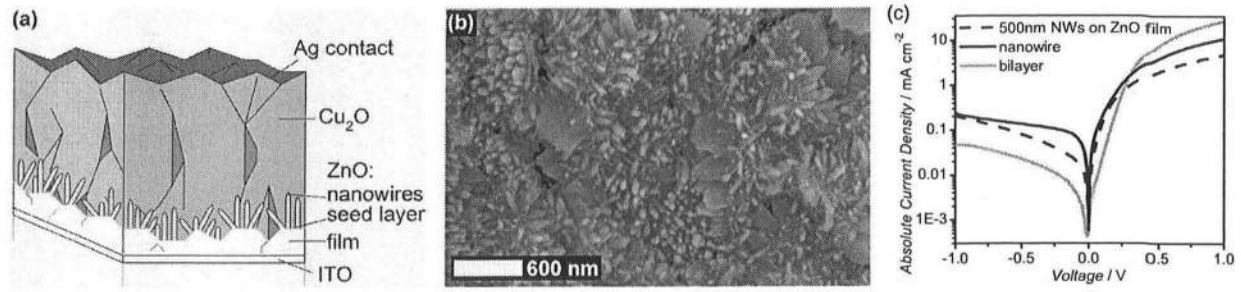

Figure 3. a) Schematic diagram of the Cu_2O-ZnO solar cell architecture used to show that leakage paths through the thin ZnO seed layer are not responsible for the low V_{OC} of the NW cells. ZnO NWs were grown on top of a ZnO film identical to that used in the bilayer devices. b) Top-down SEM image of ZnO NWs grown on a ZnO film. c) Dark current densities measured for the device architecture shown in (a), as well as the bilayer and NW cells from Figure 1.

Table 1. V_{OC} of Cu_2O-ZnO NW solar cells with different nominal NW lengths and 3 μm Cu_2O absorbing layers.

Nominal NW length [nm]	V_{OC} [V]
575	0.19 ± 0.01
1000	0.19 ± 0.01
1250	0.22 ± 0.01

attributable to shunt pathways through the ZnO seed layer that are reduced with further NW coverage. At forward biases, the devices with different NW lengths show similar dark current densities. Notably, at small positive biases, the dark currents are much larger than that of the bilayer device in Figure 3c. It is noted that while the dark current might be expected to scale with interface area/NW length, the size of the NWs is also likely to affect the nucleation and properties of the surrounding Cu_2O (density of grain boundaries, crystalline perfection, etc.), which influence the dark current. Thus, while further characterization is necessary to better understand what determines the dark current density of the NW cells, the absence of a strong correlation between NW length and dark current suggests that the larger interface is not primarily responsible for the lower V_{OC} observed in the NW devices.

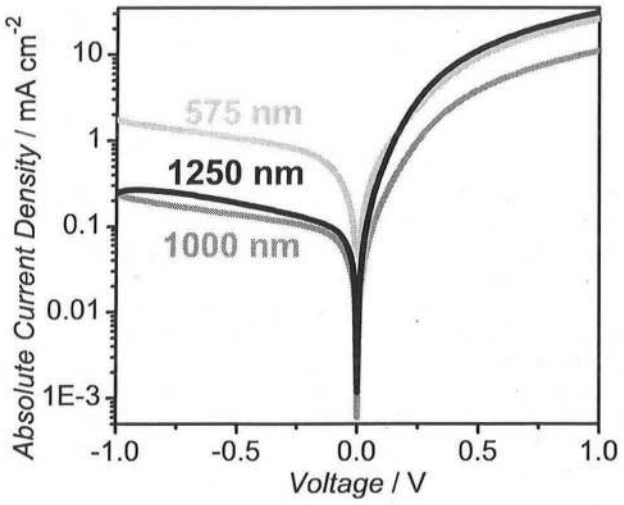

Figure 4. Dark current densities measured for NW devices with approximately 3 μm of Cu_2O and different nominal NW lengths.

Interface states are also expected to influence the V_{OC} of heterojunction solar cells and the density of such states is likely to vary for bilayer and NW architectures. In a recent report we showed that the low V_{OC} in electrodeposited Cu_2O-ZnO cells can be attributed, in part, to a high density of these states, which act as recombination centers at the solution-processed heterojunction, and the V_{OC} of the NW cells was improved to 0.28 V by using a buffering technique to limit interface state formation.[16] The buffering method eliminated the annealing requirement of the NW cells such that the synthesis method was identical to that of the bilayer devices studied here. Nonetheless, the value of 0.28 V is still well below that of comparable bilayer devices.

Thus while factors such as leakage currents, heterojunction area, annealing treatments, and interface states will definitely influence the properties of these solution-processed heterojunctions (to varying degrees in the bilayer and NW architectures), none appear to be the major cause of the low V_{OC} observed in the NW cells. Further studies to understand the disparity in the V_{OC} values of the NW and bilayer devices focus on the formation of the built-in bias in Cu_2O layers of varying thickness.

2.2. Influence of Cu_2O Thickness on V_{OC}

Figure 5 displays the V_{OC} values of bilayer and NW heterojunctions under AM1.5G illumination as a function of the thickness of the Cu_2O layer. The NW cells had 1 μm nominal NW lengths. Dark current density measurements of these devices are included in the Supporting Information.

For the bilayer devices, the V_{OC} is observed to be roughly constant at Cu_2O thicknesses greater than approximately 2.8 μm, but falls sharply for thinner Cu_2O layers. The built-in bias of the heterojunction, which opposes the flow of undesirable dark current and provides an open-circuit voltage, results from the diffusion of electrons in the n-ZnO to the p-Cu_2O. Depletion layers are produced in both materials at the heterointerface and components of the built-in bias, $V_{bi}(n)$ and $V_{bi}(p)$, are formed in the ZnO and Cu_2O respectively, as shown in Figure 2c.

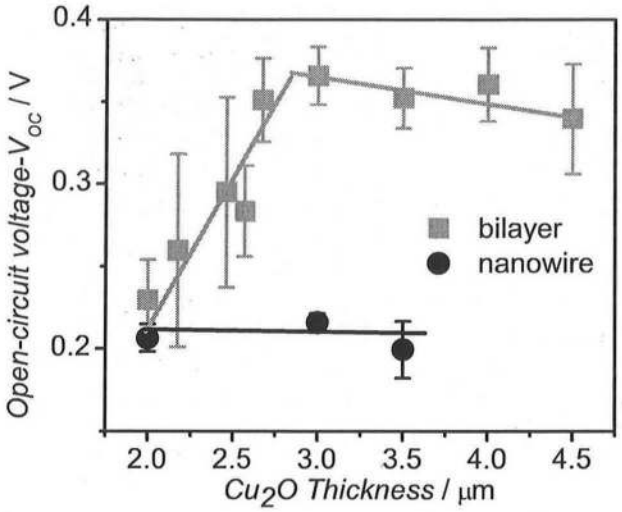

Figure 5. Measured V_{OC}'s of bilayer and NW Cu_2O-ZnO cells with different Cu_2O thicknesses. Three devices were measured for each Cu_2O thickness and the standard deviation is given by the error bounds. Lines have been added as guides for the eye.

Application of Poisson's equation at the interface gives the following ratio for these components of the built-in potential:

$$\frac{V_{bi}(n)}{V_{bi}(p)} = \frac{N_A \varepsilon_{Cu_2O}}{N_D \varepsilon_{ZnO}} \quad (1)$$

where N_D, N_A, ε_{ZnO}, and ε_{Cu2O} are the net donor and acceptor doping densities and absolute permittivities in the ZnO and Cu_2O respectively.[20] The carrier densities of electrodeposited Cu_2O and ZnO are typically on the order of 10^{13}–10^{14} cm^{-3} and 10^{18}–10^{20} cm^{-3} respectively.[21–23] Hall measurements on the Cu_2O films used here indicated a carrier density (N_A) of approximately 6×10^{13} cm^{-3}. Thus it follows from Equation 1 that almost the entire built-in bias of the heterojunction is formed in the Cu_2O layer ($\varepsilon_{Cu_2O} = 6.2$, $\varepsilon_{ZnO} = 8.0$).[24]

Furthermore, an expression of the form:

$$V_{bi}(p) = \frac{q N_A x_p^2}{2 \varepsilon_{Cu_2O}} \quad (2)$$

can be used to estimate x_n and x_p, the thickness of the depletion layer in the ZnO and Cu_2O, where q is the electron charge. Equation 2 indicates that for an expected built-in bias in the range of 0.4 to 0.7 V, the depletion layer thickness in the Cu_2O (x_p) is approximately 2.3 to 3.0 μm. This calculated depletion layer thickness matches well with the Cu_2O thickness in the bilayer devices in Figure 5 at which the V_{OC} was observed to decrease sharply. This suggests that the drop in V_{OC} for thinner devices is due to the inhibition of the full built-in bias. These results are in agreement with low V_{OC} and V_{bi} values reported previously for Cu_2O-ZnO heterojunctions utilizing thin Cu_2O layers.[21,25,26] The authors of these studies did not, however, identify the inhibited depletion layer formation as a possible cause of the low V_{OC} values they observed. Heterojunctions reporting more substantial values of V_{OC} and V_{bi} have used Cu_2O layers thicker than 2 μm.[13,14,16,27,28] A heterojunction employing a 1.8 μm thick sputtered Cu_2O layer also demonstrated a reasonable built-in bias of approximately 0.4 V.[29] The sputtered Cu_2O layer had a higher carrier density than electrodeposited Cu_2O (approximately 10^{16} cm^{-3}), such that a smaller depletion layer thickness (approximately 200 nm) would be expected.

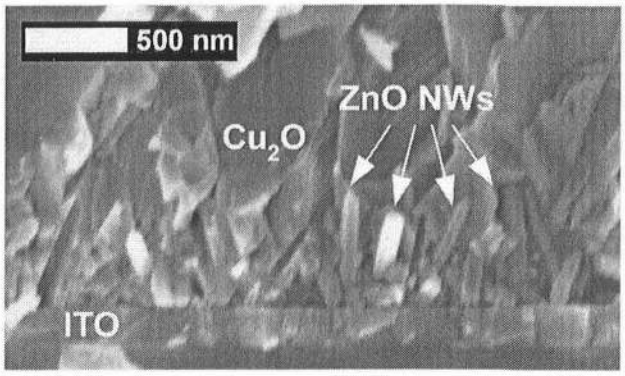

Figure 6. SEM cross-section of a Cu_2O-ZnO NW cell from this study. The ZnO NW spacing is much less than the Cu_2O thickness required for formation of the full built-in bias, resulting in local shunting, increased recombination, and a lower V_{OC}.

V_{OC} values of approximately 0.20 V are observed for the NW cells in Figure 5, regardless of the Cu_2O thickness, similar to that of the depleted bilayer devices. The formation of the depletion layer is expected to be problematic in nanostructured Cu_2O heterojunctions. As shown in **Figure 6**, the spacing between adjacent wires in the NW cells is only a few hundred nanometers. It is therefore expected that the full V_{bi} cannot be achieved and regions of local shunting will result. These results strongly suggest that inhibited depletion layer formation is largely responsible for the low V_{OC} in the NW cells.

In seeming contradiction, V_{OC}'s above 0.5 V were recently reported for electrodeposited Cu_2O-ZnO NW cells under AM1.5G illumination.[17] However, those devices also exhibited small J_{SC}'s (substantially less than that of simple bilayer devices), suggesting a different photovoltaic mechanism may be involved. The devices were annealed at a temperature of 300 °C, for which the oxidation of Cu_2O to CuO in the bulk may occur and the formation of Cu at the Cu_2O-ZnO interface is thermodynamically expected, suggesting that a Cu_2O/Cu/ZnO architecture may result.[12,30] This is consistent with the recent observation of excellent rectification in an electrodeposited Cu_2O/Cu/ZnO heterostructure.[31]

It is recognized that a large interface state density can influence the built-in potential of a heterojunction and the expected depletion layer thickness. Thus while the importance of the Cu_2O thickness will depend on the material and interfacial conditions of the particular heterojunction, the results and calculations presented here demonstrate that a fundamental discrepancy between the periodicity of the NWs and the desired heterojunction thickness can exist. This has important implications for the design of Cu_2O-ZnO heterojunctions for photovoltaics, photodetectors,[32,33] and fundamental studies of charge dynamics.[34,35] **Figure 7** shows that an increase in the Cu_2O carrier density of at least two orders of magnitude will be necessary

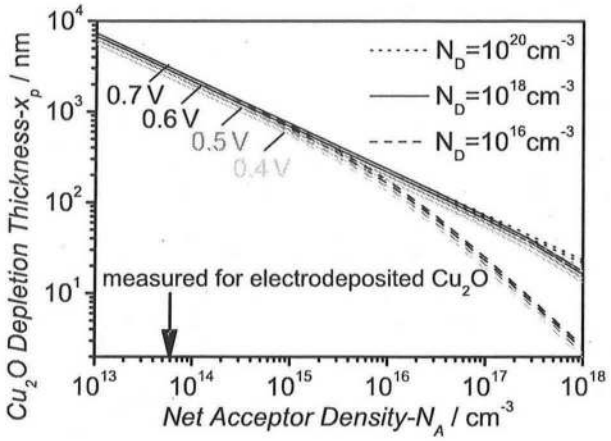

Figure 7. Estimated Cu_2O depletion layer thickness (x_p) as a function of net acceptor density in the material (N_A) for three different carrier concentrations in the ZnO (N_D) and a range of relevant built-in biases.

to achieve a depletion layer thickness compatible with the nanostructured architecture used here. Future studies of nanostructured Cu_2O-ZnO heterojunctions with variable carrier densities and nanostructure spacing will allow detailed investigation of this relationship.

2.3. Influence of Cu_2O Thickness on J_{SC}

Figure 8a shows the J_{SC}'s of the same bilayer and NW devices as in Figure 5. Observed J_{SC}'s are consistent with inhibited depletion layer formation in the Cu_2O. In previous work, we calculated the amount of current that can be harvested from various thicknesses of Cu_2O under 100 mW cm^{-2} AM1.5G illumination, assuming no reflection or scattering effects.[3] The J_{SC}'s of the bilayer devices in Figure 8a are less than 4 mA cm^{-2}, well below the approximately 6 mA cm^{-2} of current that we might expect to collect from a single micron of Cu_2O. This strongly suggests that the minority carrier collection lengths in the devices presented here are less than 1 μm. In the Cu_2O, electrons that are photogenerated at distances greater than 1 μm from the Cu_2O-ZnO interface recombine before they can be collected. This is in agreement with a Cu_2O minority carrier collection length of 430 nm calculated recently using a 1D transport model.[36] Application of a drift collection model to external quantum efficiency spectra of the devices studied here likewise indicated collection lengths below 1 μm.[37] Thus it is expected that any Cu_2O beyond a thickness of 1 μm does not contribute to the photocurrent, but might reduce beneficial optical confinement effects[38] and add a series resistance. Despite this, the J_{SC} of the bilayer devices is seen to increase with Cu_2O thickness in Figure 8a for thicknesses up to approximately 3 μm. This can be attributed to an increase in the built-in bias with increasing Cu_2O thickness. Calculations from the previous section suggest that the internal drift field may increase with Cu_2O thickness up to approximately 3 μm, increasing the minority carrier collection length, albeit still to a value less than 1 μm. For Cu_2O thicknesses greater than 3 μm, no increase in the charge-collecting field is expected (the full built-in bias has already been formed), and holes must travel further through the Cu_2O to be collected. Coupled with reduced optical confinement effects, this results in a decrease in the J_{SC}.

In contrast, the J_{SC} of the NW cells decreases when Cu_2O thickness is increased from 2 μm, albeit from a higher starting value, as inhibition of the depletion layer likely prevents any increase in the internal drift field. The additional Cu_2O only reduces optical confinement in the charge collection region and increases the travel distance to the electrode for the holes. As a result, the maximum η for the bilayer cells is observed in Figure 8b to occur at a Cu_2O thickness of approximately 3 μm, in agreement with the highest efficiency previously reported for electrodeposited devices.[14] Conversely, the NW device with the thinnest 2 μm Cu_2O layer is slightly more efficient than the thicker NW devices, although the optimal Cu_2O thickness will certainly vary with NW length.

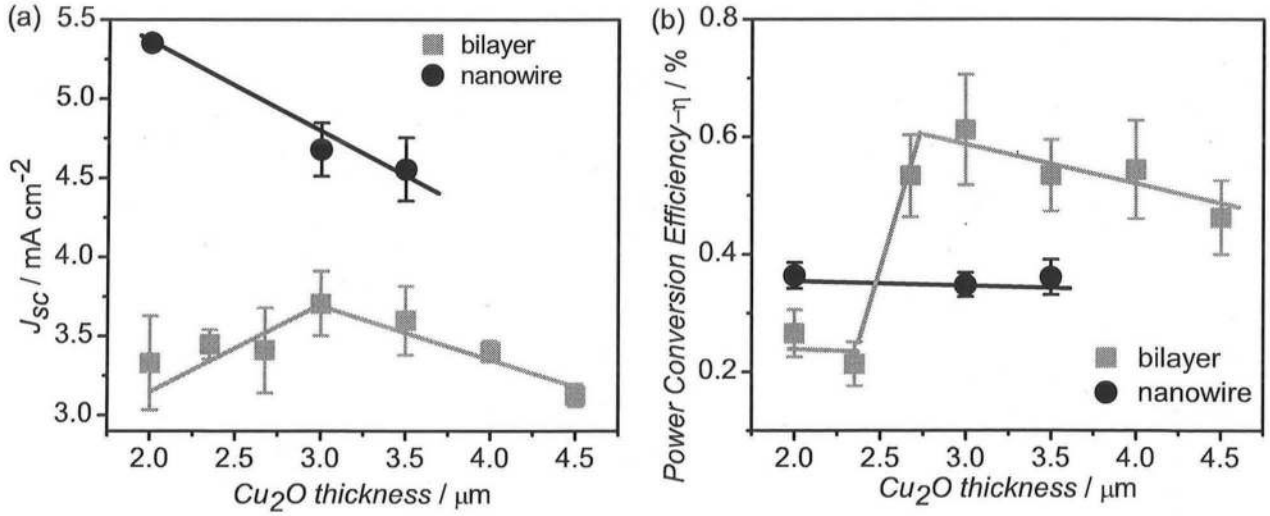

Figure 8. Measured a) J_{SC}'s and b) η of bilayer and NW Cu_2O-ZnO cells with different Cu_2O thicknesses. The NW cells had NWs with 1 μm nominal length.

Due to the thick depletion layer in bilayer devices, the predominant carrier transport mechanism in the light-absorbing Cu_2O is drift. This has not been widely recognized in the literature, with poor transport previously attributed to short electron *diffusion* lengths in Cu_2O. Only recently did Jeong et al. note that the low carrier concentration of electrodeposited Cu_2O may result in thin layers of Cu_2O being fully depleted.[35] Conversely, the negligible depletion layer thickness in the ZnO means that carriers created in the ZnO by UV absorption are collected by a diffusive process.

3. Conclusions

Through this systematic study of nanostructured and bilayer architectures, a greater understanding of the underlying device physics and of the fundamental limitations of electrodeposited Cu_2O-ZnO solar cells has been achieved. Low electron mobilities in electrodeposited Cu_2O inhibit charge collection from bilayer device structures. While NWs can be used to improve minority carrier collection in all-oxide PV, low V_{OC}'s typically result. Studies of these cells as a function of the ZnO NW seed layer and NW length indicated that while leakage currents and interface area are important to consider, they do not appear to be primarily responsible for the low V_{OC}'s observed in the NW cells.

Through study of the devices as a function of Cu_2O thickness, it was demonstrated that a fundamental limitation in the V_{OC} of nanostructured Cu_2O-ZnO heterojunctions may arise from a disparity in operating length scales. A depletion layer approximately 2.7 to 3.0 μm thick was experimentally shown (supported by theoretical calculations) to exist in the Cu_2O of the bilayer devices studied here, owing to the low carrier density of electrodeposited Cu_2O. While the achievable built-in bias of the NW cells may differ somewhat due to changes in the material and interface properties induced by the NWs, it is clear that the distance of a few hundred nanometers between the ZnO NWs, so chosen to improve charge collection, is insufficient to form a comparable Cu_2O depletion layer. Interfacial barrier layers, optimization of the nanostructure geometry, and a reduction in recombination center density are all routes to improving the V_{OC}. However this work suggests that enabling the full built-in bias at nanostructured interfaces may be essential to achieving V_{OC}'s similar to those in comparable bilayer solar cells. This need to control the depletion width, relative to the nanostructure size, has been similarly noted for silicon solar cells.[39]

The lack of other light-absorbing p-type oxides makes Cu_2O doping and mobility enhancement important areas for future investigation. It was shown that an increase in the Cu_2O carrier density of more than an order of magnitude is necessary to reduce the depletion thickness to a value smaller than the minority carrier collection length (<1 μm). Such doping of Cu_2O has been reported by physical vapor deposition methods but not, to our knowledge, by electrochemical means that are suitable for the synthesis of low-cost nanostructured heterojunctions.[29,40,41] Alternatively, mobility improvements in electrodeposited Cu_2O could result in charge collection lengths greater than the depletion thickness (>2 μm), alleviating the need for closely spaced nanostructures. Although heterojunctions have been studied in this work, similar implications hold for homojunction architectures, which will be necessary if efficiencies approaching the theoretical limit are to be achieved.

Thus while electrodeposited nanostructured all-oxide photovoltaics are promising as ultra-low-cost solar cells, it is clear from this work that fundamental limitations must be addressed. Improvements in the electrical and morphological properties of the nanostructured oxide materials are required to simultaneously achieve efficient charge collection and a high resistance to recombination in this class of devices.

4. Experimental Section

Device Synthesis: Bilayer and NW Cu_2O-ZnO cells were electrodeposited from aqueous solutions onto commercial substrates (Praezisions Glas & Optik) consisting of an approximately 200 nm thick ITO layer (sheet resistance less than 10 Ω sq^{-1}) on soda glass. All substrates were cleaned in an ultrasonic bath with acetone and isopropanol for 20 min prior to use. For the growth of ZnO NWs, a Zn seed layer was sputtered onto the substrates using an Emitech sputter coater. The Zn layer subsequently oxidized to ZnO upon immersion in the heated aqueous solution. The seed layer was approximately 50 nm thick (unless stated otherwise). The electrodepositions were performed using a standard three-electrode cell (Pt counter electrode, Ag/AgCl in saturated KCl reference electrode) and potentiostat/galvanostat under computer control as reported previously.[3,16] All chemicals used were reagent grade, and the water purified (resistivity greater than 16 MΩ cm).

ZnO nanowires were potentiostatically deposited at −1.0 V vs. Ag/AgCl from a $ZnCl_2$ (5×10^{-4} M)/KCl (0.1 M) solution at 78 °C, following previous reports.[42] Oxygen was bubbled in the solution throughout the deposition to ensure oxygen saturation. The nominal thickness of deposited ZnO was calculated by integrating the deposition current and was controlled by changing the duration of the deposition. The nominal thickness was found to roughly correspond to the length of the longest NWs deposited, as observed by SEM.

For the bilayer heterojunctions, ZnO layers with nominal thicknesses of 550 nm were potentiostatically deposited at −0.85 V vs. Ag/AgCl from a simple $Zn(NO_3)_2$ (0.08 M) solution at 70 °C, following from previous reports.[21] A 75% H_2O; 25% ethanol by volume electrolyte was recently shown to improve the macroscopic continuity of ZnO films electrodeposited in this manner by preventing the formation of hydrogen bubbles on the working electrode and corresponding pinholes in the ZnO film.[43] For the study of bilayer device properties as a function of Cu_2O thickness, the ZnO films were deposited from such a water-ethanol solution to ensure uniformity and reliable comparison amongst devices.

Cu_2O was deposited galvanostatically onto the ZnO films and NWs at −1.0 mA cm^{-2}. The Cu_2O deposition solution consisted of $CuSO_4$(0.4 M)/lactic acid(3 M) at 40 °C, to which NaOH(4 M) was added to adjust the pH to approximately 12.5.[14] For the study of bilayer device properties as a function of Cu_2O thickness, the Cu_2O depositions were performed using a solution buffered with ZnO powder, which we recently showed improved the Cu_2O-ZnO interface by preventing ZnO dissolution in the basic electrolyte.[16]

For the deposition of both the ZnO and Cu_2O films, the nominal film thicknesses were again calculated by monitoring the deposition current and were found to correspond closely to the actual film thicknesses (as observed by SEM), indicating a high Faradaic efficiency for both of these deposition methods. The thickness of the Cu_2O absorbing layer was varied by adjusting the duration of the galvanostatic deposition.

Gold or silver contacts (0.125 cm^2) were evaporated onto the Cu_2O to form an ohmic contact. As reported previously, the NW cells showed little photovoltaic behavior in their as-deposited form and require annealing at moderate temperatures for several hours.[16] It was shown that by employing the aforementioned buffering technique to limit the formation of defect states at the Cu_2O-ZnO NW interface during synthesis, the annealing treatment could be avoided and photovoltaic

behavior was observed after the devices sat in air for several days, presumably during which some passivation of defect states occurred. As the influence and reproducibility of the air exposure time is not yet suitably characterized, the NW cells in this work were annealed for 4 h at 100 °C to allow reliable comparison amongst the devices. Bilayer devices, on the other hand, show reliable photovoltaic performance without annealing, which was credited to a smaller density of interface states at the smoother heterojunction.[16] As these junctions are intended as low-cost devices that can be synthesized on a variety of low-cost substrates, thermal treatments were avoided where possible and thus the bilayer devices were measured in their as-deposited form in this study.

Device Characterization: Dark and AM1.5G current density-voltage measurements were performed using a Keithley 2400 SourceMeter with a custom-made LabView program. Solar simulators equipped with AM1.5G filters were used at 100 mW cm^{-2} intensity. The intensity was calibrated using silicon reference diodes certified by VLSI Standards Inc. or ISE Fraunhofer Institute. It is important to exercise caution when relating dark current density measurements to device performance for these devices as both ZnO and Cu_2O are photoconductive, such that the properties of the heterojunction can vary significantly with illumination. Dark current measurements were performed following illumination. Scanning electron microscopy images were obtained using a LEO VP-1530 field emission SEM. Hall measurements were performed in a magnetic field swept from –500 mT to 500 mT at constant current and temperature. For Hall measurements, Cu_2O was electrodeposited directly on ITO then transferred to a non-conducting glass substrate using an epoxy liftoff technique described previously.[44]

Supporting Information

Supporting Information is available from the Wiley Online Library or from the author.

Acknowledgements

The authors acknowledge the International Copper Association and the German Research Foundation (DFG)- Cluster of Excellence "Nanosystems Initiative Munich (NIM)" for funding. K.P.M. also acknowledges the Natural Sciences and Engineering Research Council of Canada, Peterhouse (Cambridge), and Girton College (Cambridge) for financial support. A.M. acknowledges the Gates Cambridge Trust. This work was enabled by an Academic Research Collaboration Grant from the British Council Germany and DAAD.

[1] K. P. Musselman, L. Schmidt-Mende, *Green* **2011**, *1*, 7.
[2] C. Wadia, A. P. Alivisatos, D. M. Kammen, *Environ. Sci. Technol.* **2009**, *43*, 2072.
[3] K. P. Musselman, A. Wisnet, D. C. Iza, H. C. Hesse, C. Scheu, J. L. MacManus-Driscoll, L. Schmidt-Mende, *Adv. Mater.* **2010**, *22*, E254.
[4] T.-J. Hsueh, C.-L. Hsu, S.-J. Chang, P.-W. Guo, J.-H. Hsieh, I.-C. Chen, *Scr. Mater.* **2007**, *57*, 53.
[5] B. D. Yuhas, P. Yang, *J. Am. Chem. Soc.* **2009**, *131*, 3756.
[6] J. Cui, U. J. Gibson, *J. Phys. Chem. C* **2010**, *114*, 6408.
[7] H. Wei, H. Gong, Y. Wang, X. Hu, L. Chen, H. Xu, P. Liu, B. Cao, *CrystEngComm* **2011**, *13*, 6065.
[8] B. Rai, *Sol. Cells* **1988**, *25*, 265.
[9] J. Nelson, *The Physics of Solar Cells*, Imperial College Press, London, UK **2003**.
[10] S. Ishizuka, K. Akimoto, *Appl. Phys. Lett.* **2004**, *85*, 4920.
[11] Y. Tsur, I. Riess, *Phys. Rev. B* **1999**, *60*, 8138.
[12] L. Papadimitriou, N. A. Economou, D. Trivich, *Sol. Cells* **1981**, *3*, 73.
[13] A. Mittiga, E. Salza, F. Sarto, M. Tucci, R. Vasanthi, *Appl. Phys. Lett.* **2006**, *88*, 163502.
[14] M. Izaki, T. Shinagawa, K. T. Mizuno, Y. Ida, M. Inaba, A. Tasaka, *J. Phys. D: Appl. Phys.* **2007**, *40*, 3326.
[15] T. Minami, Y. Nishi, T. Miyata, J. Nomoto, *Appl. Phys. Express* **2011**, *4*, 062301.
[16] K. P. Musselman, A. Marin, A. Wisnet, C. Scheu, J. L. MacManus-Driscoll, L. Schmidt-Mende, *Adv. Funct. Mater.* **2011**, *21*, 573.
[17] J.-W. Chen, D.-C. Perng, J.-F. Fang, *Sol. Energy Mater. Sol. Cells* **2011**, *95*, 2471.
[18] N. O. V. Plank, M. E. Welland, J. L. MacManus-Driscoll, L. Schmidt-Mende, *Thin Solid Films* **2008**, *516*, 7218.
[19] B. M. Kayes, H. A. Atwater, N. S. Lewis, *J. Appl. Phys.* **2005**, *97*, 114302.
[20] A. G. Milnes, D. Feucht, *Heterojunctions and metal-semiconductor junctions*, Academic Press, New York, USA **1972**.
[21] J. Katayama, K. Ito, M. Matsuoka, J. Tamaki, *J. Appl. Electrochem.* **2004**, *34*, 687.
[22] K. Mizuno, M. Izaki, K. Murase, T. Shinagawa, M. Chigane, M. Inaba, A. Tasaka, Y. Awakura, *J. Electrochem. Soc.* **2005**, *152*, C179.
[23] I. Mora-Sero, F. Fabregat-Santiago, B. Denier, J. Bisquert, R. Tena-Zaera, J. Elias, C. Levy-Clement, *Appl. Phys. Lett.* **2006**, *89*, 203117.
[24] *Springer Materials - The Landolt-Bornstein Database, Inorganic Solid Phases - Physical Properties*, (Eds: Y. Gorelenko, P. Villars), Springer-Verlag GmbH, Heidelberg, Germany **2008**.
[25] M. Izaki, K. Mizuno, T. Shinagawa, M. Inaba, A. Tasaka, *J. Electrochem. Soc.* **2006**, *153*, C668.
[26] S.-M. Chou, M.-H. Hon, I.-C. Leu, Y.-H. Lee, *J. Electrochem. Soc.* **2008**, *155*, H923.
[27] D. K. Zhang, Y. C. Liu, Y. L. Liu, H. Yang, *Physica B* **2004**, *351*, 178.
[28] S. S. Jeong, A. Mittiga, E. Salza, A. Masci, S. Passerini, *Electrochim. Acta* **2008**, *53*, 2226.
[29] S. Ishizuka, K. Suzuki, Y. Okamoto, M. Yanagita, T. Sakurai, K. Akimoto, N. Fujiwara, H. Kobayashi, K. Matsubara, S. Niki, *Phys. Status Solidi C* **2004**, *1*, 1067.
[30] J. Herion, E. A. Niekisch, G. Scharl, *Sol. Energ. Mater.* **1980**, *4*, 101.
[31] B. M. Fariza, J. Sasano, T. Shinagawa, H. Nakano, S. Watase, M. Izaki, *J. Electrochem. Soc.* **2011**, *158*, D621.
[32] R.-C. Wang, H.-Y. Lin, *Sens. Actuators, B* **2010**, *149*, 94.
[33] H. T. Hsueh, S. J. Chang, F. Y. Hung, W. Y. Weng, C. L. Hsu, T. J. Hsueh, T. Y. Tsai, B. T. Dai, *Superlattices Microstruct.* **2011**, *49*, 572.
[34] T. Jiang, T. Xie, Y. Zhang, L. Chen, L. Peng, H. Li, D. Wang, *Phys. Chem. Chem. Phys.* **2010**, *12*, 15476.
[35] S. Jeong, S. Song, K. Nagaich, S. Campbell, E. Aydil, *Thin Solid Films* **2011**, *519*, 6613.
[36] Y. Liu, H. K. Turley, J. R. Tumbleston, E. T. Samulski, R. Lopez, *Appl. Phys. Lett.* **2011**, 98.
[37] K. P. Musselman, T. Gershon, J. L. MacManus-Driscoll, R. H. Friend, unpublished.
[38] T. Gershon, K. Musselman, A. Marin, R. H. Friend, J. L. MacManus-Driscoll, *Sol. Energy Mater. Sol. Cells* **2012**, *96*, 148.
[39] L. Tsakalakos, J. Balch, J. Fronheiser, B. A. Korevaar, O. Sulima, J. Rand, *Appl. Phys. Lett.* **2007**, *91*, 233117.
[40] S. Ishizuka, S. Kato, Y. Okamoto, K. Akimoto, *J. Cryst. Growth* **2002**, *237–239*, 616.
[41] S. Suzuki, T. Miyata, T. Minami, *J. Vac. Sci. Technol. A* **2003**, *21*, 1336.
[42] J. Elias, R. Tena-Zaera, C. Levy-Clement, *J. Electroanal. Chem.* **2008**, *621*, 171.
[43] K. P. Musselman, T. Gershon, L. Schmidt-Mende, J. L. MacManus-Driscoll, *Electrochim. Acta* **2011**, *56*, 3758.
[44] M. Miyake, K. Murase, T. Hirato, Y. Awakura, *J. Electrochem. Soc.* **2003**, *150*, C413.